Asian Journal of Chemistry; Vol. 33, No. 3 (2021), 632-636

ASIAN JOURNAL OF CHEMISTRY

https://doi.org/10.14233/ajchem.2021.23076

Microencapsulation of Gadolinium Citrate using Silica for Contrast Agent Development

A. SEPTIANI, A. ANGGRAENI, A. HARDIANTO, D.R. EDDY* and H.H. BAHTI

Department of Chemistry, Faculty of Mathematics and Natural Sciences, Universitas Padjadjaran, Jl. Raya Bandung-Sumedang km. 21 Jatinangor, Sumedang, West Java 45363, Indonesia

*Corresponding author: Fax: +62 22 7794-391; Tel: +62 8132 2731173; E-mail: diana.rahmawati@unpad.ac.id

Received: 21 November 2020; *Accepted*: 16 January 2021; *Published online*: 16 February 2021; AJC-20261

Gadolinium is a potential T_1 contrast agent because it provides a better image for magnetic resonance imaging (MRI). However, as toxic gadolinium ions can be released from the coordination compounds, it is often encapsulated using silica. Silica-encapsulated gadolinium citrate is a colloid, therefore, encapsulation efficiency should be determined by the standard addition method, not the external standard, to minimize errors in the matrix. Silica-encapsulated gadolinium citrate (Gd-$C_6H_5O_7$@SiO_2) was prepared *via* the Stöber sol-gel method by mixing gadolinium citrate, ethanol, aqua proinjection, tetraethylorthosilicate (TEOS) and ammonia, then the encapsulation efficiency was determined using the standard addition method. Particle size analysis revealed that the average size of Gd-$C_6H_5O_7$@SiO_2 particles was 1.53 μm having a encapsulation efficiency of 90.44%.

Keywords: Gadolinium, Microencapsulation, Silicon dioxide, Magnetic resonance imaging.

INTRODUCTION

Cancer occurs due to mutations in cellular DNA, thereby causing the abnormal growth and proliferation of cells, which can spread throughout the body *via* the blood vessels and lymph vessels [1]. Typically, magnetic resonance imaging (MRI), a non-invasive diagnostic technique, is used to produce high-resolution anatomical images of soft tissue, thereby providing a quantitative assessment of disease pathogenesis [2]. This technique requires contrast agents with paramagnetic properties which differentiate between normal tissue and the diseased tissue by modulating their intrinsic contrast [3]. Paramagnetic properties are the choice in cancer detection because of their high sensitivity and selectivity. This ability is possessed by rare earth metals such as gadolinium.

However, gadolinium can be nephrotoxic at high doses (> 0.3 mmol/kg), causing transient albuminuria and enzyme excretion in urine in the kidneys [4]. These problems can be overcome by forming gadolinium coordination compounds with certain chelates, such as DOTA (also known as tetraxetan) [5] or a combination of gadolinium silica [6]. Eddy *et al.* [7] reported that mesoporous gadolinium silica still contained Gd^{3+} (3.56×10^{-3} mg), releasing 6.32×10^{-2} mg free gadolinium ions. The release of such toxic ions can be overcome by encapsulation with an inorganic material [8] to form a colloid. However, the colloid can scatter light, causing the measured encapsulation efficiency to be quite low, approximately 75.24%. In the external standard method, the standard solution matrix is not the same as the colloid sample, thus, a more suitable method for determining the encapsulation efficiency is a standard addition, which overcomes the complexity of the sample matrix because the sample and standard are in the same condition [9].

The reported low encapsulation efficiency is presumed to be low due to the inaccuracy of the efficiency test method. The study of Gd-$C_6H_5O_7$@SiO_2 synthesis and measurement of encapsulation efficiency by standard addition method can be used as a reference for contrast agent synthesis. Moreover, no free gadolinium ions would be generated and further tests can be conducted to utilize Gd-$C_6H_5O_7$@SiO_2 as a cancer-selective contrast agent.

EXPERIMENTAL

The chemicals used in this study were alizarin red S, 25% ammonia (NH_4OH), glacial acetic acid, aqua proinjection, 100% ethanol, gadolinium(III) chloride hexahydrate ($GdCl_3 \cdot 6H_2O$) sodium acetate buffer solution having pH 3.5

(CH_3COONa), sodium hydroxide (NaOH), trisodium citrate ($Na_3C_6H_5O_7$) and tetraethylorthosilicate 99% (TEOS) were procured from Merck and used without further purification.

The synthesis was based on Stöber's method in the presence of gadolinium ions protected by citrate ions [9], observation of the encapsulation process, characterization of Gd-$C_6H_5O_7$@SiO_2 microcapsules and determination of the efficiency (%) of encapsulated Gd-$C_6H_5O_7$@SiO_2 were performed using standard addition methods.

Synthesis of Gd-$C_6H_5O_7$@SiO_2: A stock solution of gadolinium citrate was prepared by mixing 200 µL of 0.5 M $GdCl_3 \cdot 6H_2O$ and 200 µL of 1 M trisodium citrate followed by the addition of 300 µL of 1.47 M NH_4OH. The solution was homogenized, then 200 µL was added to 7.5 mL of aqua proinjection and 17.5 mL of ethanol. Next, 50 µL of TEOS was added to the stirred solution at room temperature for 5 min, before the addition of 740 µL of ammonia (25%) and stirring was continued for 16 h at room temperature.

Encapsulation efficiency determination by standard addition: Samples of the synthesized Gd-$C_6H_5O_7$@SiO_2 (0, 0.3, 0.35, 0.45 and 0.6 mL) were added to 25 mL volumetric flasks, before the addition of 1000 ppm of the standard solution of gadolinium standard and 0.2 M acetic acid to achieve pH 3.5. Then, 3 drops of pH 3.5 sodium acetate buffer and 1000 ppm alizarin red S were added followed by the addition of aqua proinjection and finally the mixture was homogenized. The absorbance of the solutions was measured and the data plotted (absorbance *versus* the standard addition volume) to obtain the intercept value to determine the concentration of free gadolinium and encapsulation efficiency as follows:

$$[Gd(III)] \text{ in sample} = -X_{intercept} \frac{C_{std}}{V_o} \quad (1)$$

$$\text{Efficiency encapsulation (\%)} = \frac{Gd_{added} - \text{Free } Gd_{after\ synthesis}}{Gd_{added}} \quad (2)$$

Detection of Gd-$C_6H_5O_7$@SiO_2 colloid: The size of the Gd-$C_6H_5O_7$@SiO_2 colloid particles was measured using an SZ-100 Horiba. The run duration was set at 60 s, using an ND filter and gate time of 100% and 2.56 µs. The form distribution applied for the calculation of particle size was polydisperse.

RESULTS AND DISCUSSION

Gadolinium in the form of gadolinium citrate complex was used to assist the sol-gel process by the citrate route. The sol-gel method by citrate route is a relatively simple method to obtain stable precursors, which have been used in the production of various oxides [10]. The experimental stage was continued with the development of Gd-$C_6H_5O_7$@SiO_2 using Stöber's method, as it can easily control the particle size with good precision and monodispersion of the particle size distribution. The particle size was controlled by adjusting the concentrations of TEOS, ethanol, solvent and base [11]. The process which occured at this stage is the formation of a gadolinium citrate core, followed by the formation of SiO_2 as a shell [12] (**Scheme-I**). In this study, a 1:1 mole ratio of gadolinium and citrate was formed.

According to Baggio *et al.* [13], the citrate sol-gel method forms a cross-linked core gadolinium citrate. Citrate has a high density and the rare earth elements have a high coordination number when bonded in a complex manner so that the complex structure of Gd-citrate has several possibilities depending on the reaction conditions. Under alkaline conditions, citric acid is predominantly deprotonated and acts as a multidentate ligand to crosslink with gadolinium to form complex having a coordination number of 9 [14]. The stock solution of gadolinium citrate as the core in the encapsulation process was measured by a spectrophotometer at UV wavelength, confirmed the formation of Gd-$C_6H_5O_7$@SiO_2. The reaction begins with the substitution of an alkoxy group by a hydroxide ion through a penta-coordinate transition state, then siloxane bonds are formed as a result of the condensation process [15]. At this stage, aqua proinjection functions as a solvent for the hydrolysis, ethanol as an agglomeration preventing agent and a medium that helps TEOS to form a silica gel. TEOS is the source of silica which act as a shell of gadolinium and does not form a salt in the gel, so no additional work is required to remove the salt. Ammonia functions to help the hydrolysis and condensation reactions the synthesis of gadolinium silica is optimum at pH 9 (alkaline) [16]. The pH affects the balance between the monomeric silicic acid and its deprotonated anions can be stabilized by water molecules. The balance shifts to anions with increasing pH [17]. The rate of each hydrolysis step depends on the stability of the transition rate on –OH group with OR, thus, the hydrolysis will be faster in alkaline conditions [15].

The mixture was stirred for 16 h to reduce aggregation, thereby maintaining the size of Gd-$C_6H_5O_7$@SiO_2 colloid particles, where silica particles formed on the gadolinium citrate surface as a result of a polycondensation reaction. The condensation follows the same pattern as hydrolysis, which is catalyzed

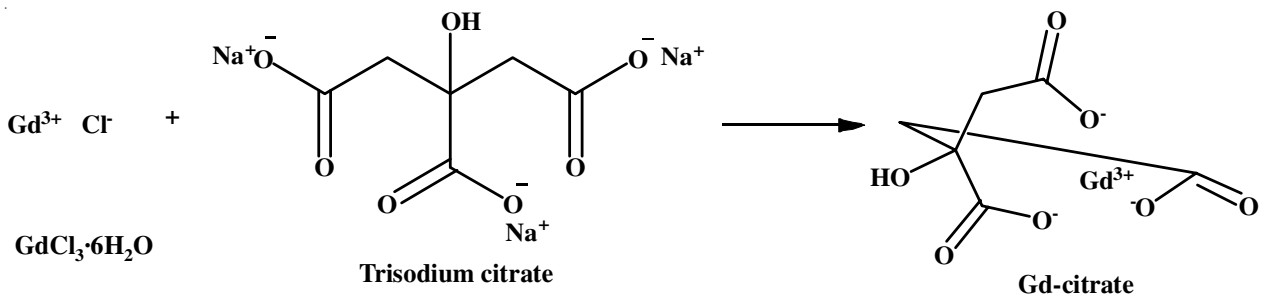

Scheme-I: Reaction of gadolinium chloride with trisodium citrate to form gadolinium citrate

by NH_4OH, to form siloxane bonds (or metalloxane bonds for other metals). Polycondensation produces small agglomerates of highly branched silica in the form of a sol, which eventually cross-links to encapsulate the gadolinium and produce colloid Gd-$C_6H_5O_7$@SiO_2. This encapsulation process was observed by measuring the UV absorbance using a UV-Vis spectrophotometer. Fig. 1 shows the different UV absorption profiles at the initial stage of gadolinium citrate as the core and after the addition of TEOS. In the first step, core gadolinium citrate was formed and the absorbance was 3.10. After the addition of TEOS, hydrolysis and condensation processes formed a silica shell and the absorbance measured at the first addition (5 min) significantly decreased to 1.618 due to silica. The addition of TEOS caused a decrease in absorbance in the 200-250 nm wavelength range. The absorbance was then measured every 30 min throughout the 16 h synthesis. After the TEOS reacted for 30 min, the absorbance was 1.25 and during the stirring (8-16 h), the absorbance showed a slight decrease to 1.183, indicating that the longer the stirring time, more SiO_2 as the encapsulator was formed, thereby improving the gadolinium citrate encapsulation efficiency (Fig. 2). The absorbance value was obtained only from the absorption on the silica surface so that it can be concluded that gadolinium citrate has been encapsulated. The higher the wavelength, the higher the frequency, which in contrast to the energy level, decreases with increasing wavelength. This energy is not sufficient to reach gadolinium citrate as it was encapsulated with silica on the surface of Gd-$C_6H_5O_7$@SiO_2.

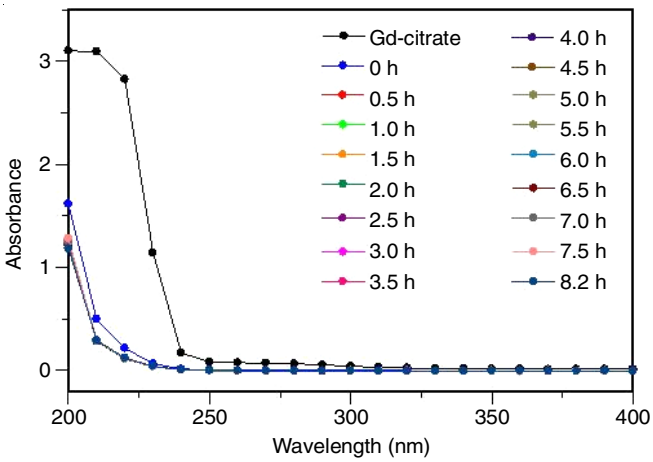

Fig. 1. Formation of Gd-$C_6H_5O_7$@SiO_2

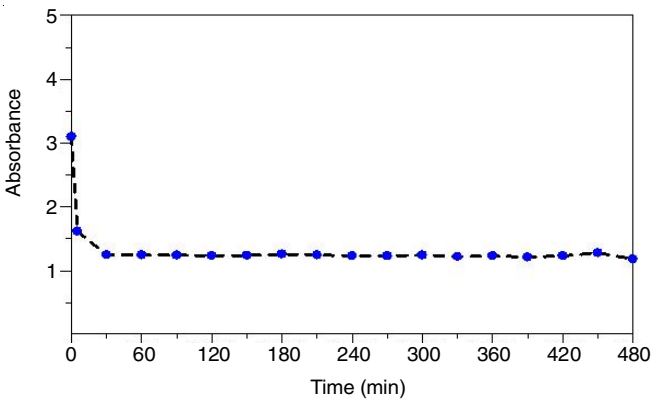

Fig. 2. Gd-$C_6H_5O_7$@SiO_2 encapsulation *versus* stirring time

Determination of particle size: Colloid Gd-$C_6H_5O_7$@SiO_2 was characterized using particle size analyzer (PSA) to determine the particle size. Fig. 3 shows one peak in the micro range, with a high percentage frequency, indicating similar-sized homogenous particles of colloid Gd-$C_6H_5O_7$@SiO_2. The peak cumulative percentage value is the particle size on the micro-scale, the average size was 1.53 µm, with a median 1.75 µm and the mode value was 1.75 µm.

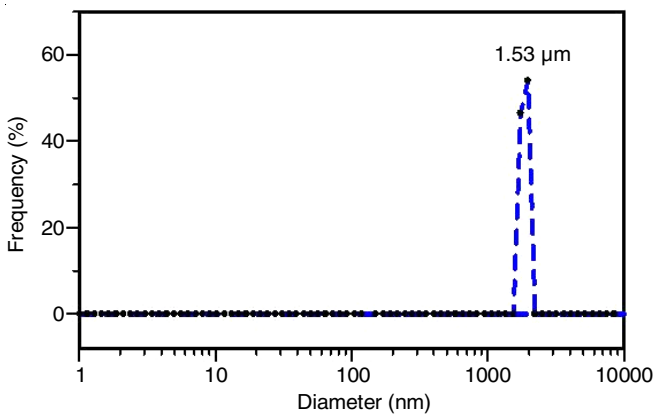

Fig. 3. Particle size characterization of Gd-$C_6H_5O_7$@SiO_2

The polydispersity index (PI) indicates the particle size distribution, with a value < 0.1 reflecting a very narrow distribution and a value > 0.7 indicating a very wide distribution of particle size, hence the possibility of agglomerates occurring in the form of sediments. The higher PI value generated, the more unstable the particles were because if the uniformity of the particles is high, the formation of flocculation and coalescence will be faster. The PI of colloid Gd-$C_6H_5O_7$@SiO_2 was 1.55, in the low-value range so the distribution range operates poorly.

Encapsulation efficiency (%) Gd-$C_6H_5O_7$@SiO_2 with standard addition: The concentration of Gd(III) that was not encapsulated in the synthesized gadolinium silica was measured to determine the encapsulation efficiency. Aqua proinjection was used as a solvent for alizarin red S, which is an indicator of the presence of Gd(III). Alizarin red S is conditioned at pH 3.5 with the addition of acetic acid or NaOH solution and sodium acetate buffer (pH 3.5) to maintain the pH since alizarin red S is stable at that pH and metals will bind to alizarin red S in the pH range 3.5-4.0. The maximum absorption wavelength of Gd-alizarin red S was determined using a visible light spectrophotometer as 530 nm and a standard addition curve of Gd-$C_6H_5O_7$@SiO_2 was generated as shown in Fig. 4.

The calibration method involved several parameters such as linearity, detection limit (LoD) and measurement limit (LoQ). A method is linear if the value of R^2 is close to 1 and in present study, the R^2 value was 0.9519. The LoD is the smallest number of analytes in the sample that can be detected and still gives a significant response compared to blank, the LoQ is the smallest quantity of analyte in a sample that can be determined with an acceptable level of precision and accuracy under agreed test

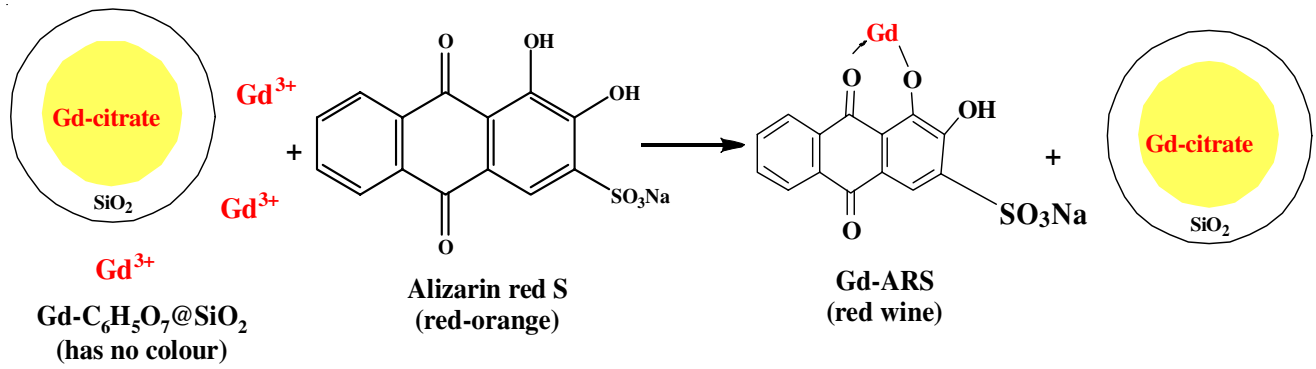

Scheme-II: Reaction of free gadolinium ions to form gadolinium-alizarin red S (ARS) complex

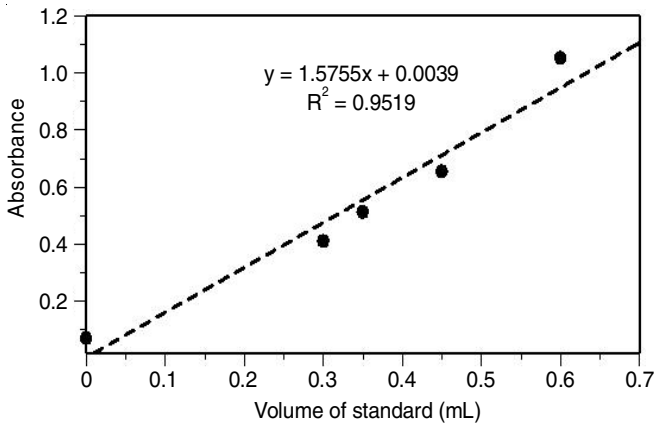

Fig. 4. Presence of Gd(III) in Gd-$C_6H_5O_7$@SiO_2 with standard addition

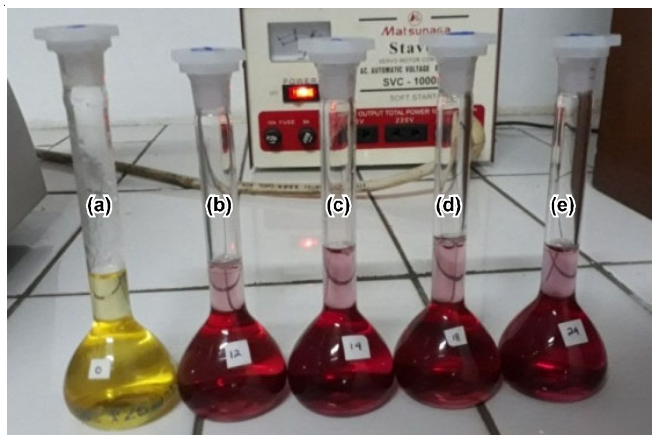

Fig. 5. Efficiency test with standard addition (a) standard addition of 0 mL, (b) 0.3 mL, (c) 0.35 mL, (d) 0.45 mL and (e) 0.6 mL

conditions and the LoL is the concentration between the quantitation limit and the point of concentration *versus* the response being non-linear. In this study, the LoD was 1.2 ppm, with an LoQ of 3.68 ppm, an LoL of a Gd-alizarin red S concentration of 26 ppm and encapsulation efficiency of 90.44% or about 8 ppm of Gd^{3+} ions still present in the sample (**Scheme-II**).

The colloid Gd-$C_6H_5O_7$@SiO_2 solution is colourless and alizarin red S is red/orange, changing to wine red when Gd(III) ions bind to alizarin red S, when the colour intensity depending on the concentration of Gd(III) ions (Fig. 5). Silica has metal adsorption ability, hence addition of alizarin red S can also confirm the formation of silica which encapsulates gadolinium citrate. If the silica formed is adsorped silica, the gadolinium will be on the silica surface, hence this gadolinium will bind to dye (such as alizarin red S) to form a complex. The colour change during the standard addition of the gadolinium standard in Fig. 5 indicates that the efficiency can be increased by the standard addition method.

Conclusion

Colloid Gd-$C_6H_5O_7$@SiO_2 was synthesized from Gd-citrate solution and TEOS *via* the sol-gel Stöber method, yielding homogenous particles with an average size of 1.53 µm and 90.44% encapsulation efficiency. The synthesized Gd-$C_6H_5O_7$@SiO_2 is a potential MRI contrast agent, however, the yield and particle size could be improved in further studies using the response surface method of Box-Behnken or central composite design.

ACKNOWLEDGEMENTS

The authors thank the Universitas Padjadjaran, Sumedang, Indonesia for providing the academic leadership grant (ALG) for support this study.

CONFLICT OF INTEREST

The authors declare that there is no conflict of interests regarding the publication of this article.

REFERENCES

1. C.L. Chaffer and R.A. Weinberg, *Science*, **331**, 1559 (2011); https://doi.org/10.1126/science.1203543
2. S. Li, J. Jiang, J. Zou, J. Qiao, S. Xue, L. Wei, R. Long, L. Wang, A. Castiblanco, N. White, J. Ngo, H. Mao, Z.R. Liu and J.J. Yang, *J. Inorg. Biochem.*, **107**, 111 (2012); https://doi.org/10.1016/j.jinorgbio.2011.11.004
3. M. Pálmai, A. Pethõ, L.N. Nagy, S. Klébert, Z. May, J. Mihály, A. Wacha, K. Jemnitz, Z. Veres, I. Horváth, K. Szigeti, D. Máthé and Z. Varga, *J. Colloid Interface Sci.*, **498**, 298 (2017); https://doi.org/10.1016/j.jcis.2017.03.053
4. H. Ersoy and F.J. Rybicki, *J. Magn. Reson. Imaging*, **26**, 1190 (2007); https://doi.org/10.1002/jmri.21135
5. L.M. Randolph, C.L.M. LeGuyader, M.E. Hahn, C.M. Andolina, J.P. Patterson, R.F. Mattrey, J.E. Millstone, M. Botta, M. Scadeng and N.C. Gianneschi, *Chem. Sci.*, **7**, 4230 (2016); https://doi.org/10.1039/C6SC00342G
6. W.I. Lin, C.Y. Lin, Y.S. Lin, S.H. Wu, Y.R. Huang, Y. Hung, C. Chang and C.Y. Mou, *J. Mater. Chem. B Mater. Biol. Med.*, **1**, 639 (2013); https://doi.org/10.1039/C2TB00283C

7. D.R. Eddy, A. Anggraeni, R.P. Fauzia, I. Rahayu, A. Mutalib, M.L. Firdaus and H.H. Bahti, *Orient. J. Chem.*, **34**, 2603 (2018); https://doi.org/10.13005/ojc/340550
8. N. Babayevska, P. Florczak, M. Wozniak-Budych, G. Nowaczyk, M. Jarek, T. Zalewski and S. Jurga, *Appl. Surf. Sci.*, **404**, 129 (2017); https://doi.org/10.1016/j.apsusc.2017.01.274
9. D.A. Skoog, D.M. West and F.J. Holler, Analytical Chemistry: An Introduction, Saunders College Publishing, Philadelphia, edn 5 (1990).
10. U. Chandra, Recent Applications in Sol-Gel Synthesis, IntechOpen, (2017).
11. X.D. Wang, Z.X. Shen, T. Sang, X.B. Cheng, M.F. Li, L.Y. Chen and Z.S. Wang, *J. Colloid Interface Sci.*, **341**, 23 (2010); https://doi.org/10.1016/j.jcis.2009.09.018
12. D.R. Eddy, A. Anggraeni, A. Hardianto, I. Rahayu and H.H. Bahti, *Chem. Res. J.*, **5**, 1 (2020).
13. R. Baggio, R. Calvo, M.T. Garland, O. Peña, M. Perec and A. Rizzi, *Inorg. Chem.*, **44**, 8979 (2005); https://doi.org/10.1021/ic0510056
14. S.K. Morcos, *Eur. J. Radiol.*, **66**, 175 (2008); https://doi.org/10.1016/j.ejrad.2008.01.025
15. A.E. Danks, S.R. Hall and Z. Schnepp, *Mater. Horiz.*, **3**, 91 (2016); https://doi.org/10.1039/C5MH00260E
16. Y.S. Lin, Y. Hung, J.K. Su, R. Lee, C. Chang, M.L. Lin and C.-Y. Mou, *J. Phys. Chem. B*, **108**, 15608 (2004); https://doi.org/10.1021/jp047829a
17. S. Wilhelm and M. Kind, *Polymers*, **7**, 2504 (2015); https://doi.org/10.3390/polym7121528